объединенный
институт
ядерных
исследований
дубна

E9-93-378

JINR TAU-CHARM FACTORY DESIGN STUDY

Submitted to «Third Workshop on the Tau-Charm Factory»,
1—6 June 1993, Marbella, Spain

1993

1 Introduction

Presently a storage ring complex project is being studied at JINR. This complex is expected to allow promising investigations in the traditional fields for Institute: elementary particle physics, nuclear physics, condensed matter physics, as well as applied investigations. The project discussed involves heavy ion storage rings with energy up to 1 GeV/nucleon, a tau-charm factory with colliding beam energy up to 2.5 GeV, a high resolution neutron source - IREN, and a synchrotron light source NK-10 with positron (electron) storage ring energy of 8-10 GeV. We plan to use JINR buildings and infrastructure as far as possible.

The tau-charm factory design is based on conservative approach, i.e. high luminosity must be obtained with principles, systems and devices tested in various scientific centres. Several variants of tau-charm factory design conception have been studied at JINR since 1991. They include conventional flat beam scheme [1], [2] and versatile magnet lattice to have the possibility of using both conventional and monochromatization schemes [3]. Recently this type of magnet lattice for tau-charm collider has been intensively studied [4],[5]. The main features of the design prepared by JINR (Dubna), SRIEA (St. Petersburg), RIPR (St. Petersburg) on the base of the versatile lattice are discussed in this paper. The beam and machine parameters and a short description of some factory systems are presented to illustrate the design feasibility.

2 Structure Scheme and Cyclograms of TCF

The layout and structure scheme of the tau-charm factory with an injection complex and the main ring are shown in Fig. 1. The injection complex consists of a preinjector and a fast booster synchrotron, where electrons and positrons are finally accelerated up to the main ring energy. The preinjector is expected to be also suitable for initial acceleration of particles for the NK-10. The energy at the preinjector output is equal to 500 MeV and the number of particles must be enough to ensure the simultaneous work of the tau-charm factory and NK-10. The injection complex cyclogram is shown in Fig. 2, where the positron flux $\dot{N}_{e^+}$ from the injection complex (a) and the luminosity time dependencies (b) are presented. The average luminosity is ensured at the level of 80 % of peak one. The beam lifetime $\tau \simeq 5$ hours is determined mainly by beam-beam bremsstrahlung radiation at the interaction point (I.P.). Due to switching time of the

detector t_{sw} =20 s the average luminosity has a maximum value for the detector counting time t_c =12 min. The positron number in the tau-charm factory must be $4.8 \cdot 10^{12}$ to get necessary luminosity value. Then taking in account that the transfer efficiency from the injection complex through the booster into the tau-charm factory is supposed to be 10%, and the filling time is chosen equal to 15 min we obtain that the productivity of the injection complex ought to be $5.4 \cdot 10^{10} e^+/s$. The positron production resolved efficiency is limited by the reasonable positron energy spread and emittance acceptable by the booster and is estimated as 0.3 %. Therefore the electron flux impinging the conversion target must be about $2 \cdot 10^{13} e^-/s$. The bunching efficiency will be of the order of 50% and the whole electron flux from the gun must be of $3.7 \cdot 10^{13} e^-/s$.

3 Booster

The booster synchrotron is designed as the injector of tau-charm factory. It will be used for acceleration of 500 MeV electrons and positrons injected from the preinjector up to the full energy of the tau-charm factory. Its circumference is of 189 m and allows to inject 15 bunches per a single turn into the main ring. With the repetition rate of 25 Hz and 2 turn injection the booster provides 0.6 A positron current to be stored in the tau-charm factory is about 15 min and the 10^{33} $cm^{-2}s^{-1}$ peak luminosity to be effectively maintained. The magnetic structure of the booster consists of 6 superperiods, each containing 6 FODO-type cells. The hexagonal shape of the booster is determined by the disposition of the injection channels in the configuration chosen for the complex. Two long straight sections house injection devices, three others are used for extraction to the injection channels of the tau-charm factory and the NK-10 booster. The sixth section houses an RF station. Each superperiod consists of 2 standard FODO cells and 4 cells with the dispersion suppressed. Positions of focusing and defocusing quadrupoles (QF, QD: l = 0.3 m, $B'_{max} = k_1 \cdot B\rho$ = 15 T/m), the H-type bending magnets (BM: l=1.3 m, B_{max} =0.84 T) and sextupoles (SD, SF: l=0.15 m, $g_{s\,max} = k_2 \cdot B\rho$ =B″/2 =50 T/m) are shown in Fig. 3 as well as the lattice functions for one superperiod. The horizontal and vertical beta functions (β_x, β_z) have extreme values of 1.8 m and 8.5 m . In the "missing magnet" region the dispersion function $D_x \leq 1$ mm, its maximum value elsewhere is D_x = 1.2 m. With a cell length of 5.25 m and tunes Q_x = 8.55 and Q_z = 8.62 a natural beam emittance $\epsilon_0 = 1.2 \cdot 10^{-7}$ m is achieved. In order to correct chromaticities ξ_x =-10.6 and ξ_z =-10.4 two sextupole families (SF and SD) will be installed near the focusing and defocusing quadrupoles. To avoid a time varying sextupole component, created due to the rising magnetic field, we suppose to use nonmetallic vacuum chambers in the dipole magnets [6]. The main booster parameters are given in Table 1.

Maximum RF voltage required for acceleration, synchrotron radiation loss compensation and obtaining of suitable bunch length σ_s is also given in Table 1.

4 Magnet Lattice of TCF

Now we have changed magnet lattice of tau-charm collider. The previous one [2] was based on conventional flat beam scheme. The new lattice [3] is versatile and allows to use both standard scheme and monochromatization one. To have the possibility to use both schemes the versatile lattice should fulfil few conditions. Two of them are of

Energy, GeV	E	2.5
Circumference, m	C	189
Emittance, m	ϵ_0	$1.2 \cdot 10^{-7}$
Tunes	Q_x/Q_z	8.55 / 8.62
Bending radius, m	ρ	9.93
Damping times, msec	$\tau_x/\tau_y/\tau_s$	9/9/4.5
Momentum compaction	α	0.0193
Energy spread	σ_E/E	$7 \cdot 10^{-4}$
Nominal current, mA	I_{e^-}/I_{e^+}	6/0.6
RF voltage, MV	V	2.5
RF frequency, MHz	f_{RF}	476
Harmonic number	q	300
Energy losses per turn, MeV	U_0	0.35
Bunch length, mm	σ_s	13.1
Repetition rate, Hz		25

Table 1: List of booster parameters

most importance. The first is a possibility to change an emittance approximately in 20 times: from 300 ÷ 400 nm for the conventional scheme up to 15 ÷ 20 nm for the scheme with monochromatization. The second is a necessity of a polarity change in micro-beta quadrupoles. The last condition is a consequence of a fact one wants to gain in energy resolution without loss of a luminosity in the case the monochromatization is made in the vertical plane.

The big change of an emittance is achieved by use of different phase advances in a regular FODO cell for conventional scheme and for monochromatization scheme and by appropriate use of wigglers. In high emittance lattice (conventional scheme) 60° phase advance is used in a regular cell. Two variants of wigglers switching to increase an emittance compared with those generated in bending magnets are now under consideration. In the first variant Robinson wigglers reduce horizontal damping partition number J_x from 1 to 0.6. Robinson wiggler consists of 4 blocks each of 0.23 m long. It is necessary to use 4 such wigglers located close to each of 4 dispersion suppressors with gradient G=4.3 T/m and magnetic field B=0.35 T. Four dipole wigglers each of 1.0 m long with magnetic field B=1.9 T, located in first half cell of suppressor, produce an additional increase of emittance. The magnetic elements location and lattice function in this variant are shown in Fig. 4. In the second variant the dipole wigglers only are used to increase an emittance. The magnetic field in dipole wigglers is 2.6 T in this case.

When comparing two variants one sees the first one is preferable from the point of view of smaller RF voltage needed to keep bunches short (see Table 2). On the other hand, in the second variant damping times are smaller and this is important for the injection and beam-beam effects. The final choice can be done after comprehensive study problems mentioned above and others such as multibunch instabilities, broadband impedance restriction etc.

For monochromatization scheme, the horizontal phase advance is 90° in a regular cell. The vertical phase advance has been chosen 45° to increase Touschek lifetime. Dipole wigglers are switched off. Robinson wigglers are switched on in a way to reduce an emittance by increasing horizontal damping partition number J_x from 1 to 2. The value of gradient in wiggler is G=7.3 T/m and magnetic field B=1.9 T. The lattice functions for low emittance lattice (monochromatization scheme) in a regular cell and dispersion suppressor are shown in Fig. 5. The dispersion suppressor is made flexible enough to cancell dispersion in both 60° lattice and 90° one.

The optical design of interaction region in conventional scheme (see Fig. 6) is modified compared with previous one [2]. To make small beta functions at interaction point $\beta_x^* = 0.30$ m and $\beta_y^* = 0.01$ m two quadrupoles are used instead of triplet. When changing polarities in quads for monochromator optics, the values of beta's become $\beta_x^* = 0.01$ m, $\beta_y^* = 0.15$ m and vertical dispersion becomes non-zero, $D_y^* = 0.36$ m. The preliminary vertical separation is made by vertical separator ES. The vertical distance between beam axes in parasitic I.P. is of $24\sigma_y$ for conventional scheme and $11\sigma_y$ for monochromatization scheme.

The change of triplet for doublet and refusal from off-axis quadrupole, located after electrostatic separator to make the vertical separation easier in previous design, is defined by condition of using of the same optical elements for both schemes. The vertical separation region was designed to make minimum of modifications when changing the scheme. To make a vertical separation easy first vertical bending magnet BV1 is located far (6 m) from electrostatic separator and the vertical beta function is minimized at its location. This allowed to keep moderate the strength of separator, $E_s = 20$ kV/cm, with the vertical distance between axes of beams at the entrance of the first vertical bending magnet $\simeq$50 mm. The vertical beam size is $\sigma_y = (\varepsilon_0\beta_y/2)^{1/2} = 0.89$ mm at this point for conventional scheme and $\sigma_y = [\varepsilon_y\beta_y + (D_y\sigma_E)^2]^{1/2}$ =0.81 mm for monochromatization scheme. Here ε_y is a vertical emittance and D_y is a vertical dispersion. With 5 mm closed orbit excursion one has more than 20 mm thickness of septum, that seems to be enough to avoid technical problems and to get tolerable magnetic field quality.

The matching of optical functions at the vertical separation region in the standard scheme is made by use of three FODO cells with vertical phase advance close to $2\pi/3$ in each. This solution gives moderate values of beta functions $\beta_{x,y}$ and gradients in quads but needs in at least 15 m between the first BV1 and the last BV3 vertical bends. The lattice functions at interaction region and vertical separation region for high emittance lattice are shown in Fig. 6.

The matching of lattice functions in the monochromatization scheme is made easier with stronger angle in the last vertical bend BV3 because of essentially non zero vertical dispersion at I.P. With vertical distance between electron and positron ring 1.2 m defined by technical requirements the short horizontal distance between vertical bends is preferable for monochromatization scheme. So, the choice of distance is made as a compromize between these two requirements. The lattice functions at the interaction region and at the vertical separation region for low emittance lattice are shown in Fig. 7.

The long straight section at opposite to I.P. side consists of FODO cells. It is used for injection of beams [7] and for location of RF cavities.

The chromaticity correction is made now for high emittance lattice [8]. Six sextupole

families with 60° phase advance per regular cell are used to correct chromatic properties. The solution have been found provides ±1.8% of energy acceptance (see Fig. 8). Variation of tunes and beta functions at I.P. for the chromaticity correction by two sextupole families and by 6 sextupole families are shown in Fig. 9, 10. The calculation of dynamic aperture has been performed with SIXTRACK code [9]. The particle considered to be stable, if it wasn't lost during N=40,000 turns. This number of turns is close to one or two damping times depending on parameters of wigglers in the lattice.

The sensitivity of lattice to errors was investigated by introducing multipole errors in dipoles and quadrupoles. Only effect of random errors on dynamic aperture was studied. For the dipole, sextupole and decapole errors have been considered. The results of tracking are presented in Fig. 11a, b, where the dynamic aperture of perfect machine is compared to the dynamic aperture in the presence of multipole errors. There is no essential effect for sextupole errors. The main effect of decapole errors occurs in the horizontal plane. This type of errors seems to be of most importance and its value is close to the design and manufacturing limit. For quadrupole, only dodecapole errors have been considered. The significant reduction of dynamic aperture is observed (Fig. 11c) with $\Delta G/G = 8 \cdot 10^{-3}$ at r=2.0 cm. This value of 12-pole component is much more than expected one.

The beam lifetime for conventional scheme is defined by beam-beam bremsstrahlung mainly. With longitudinal acceptance 1.8% and average pressure in vacuum chamber of $2 \cdot 10^{-9}$ Torr it is of 6.5 hours. The Touschek lifetime is much more, $\tau_T \simeq$90 h. The beam lifetime for monochromatization scheme is defined by Touschek effect predominatingly and depends strongly on dynamic aperture. Its estimate gives $1 \div 3$ hours [5], [10]. The main parameters of tau-charm collider are presented in Table 2.

5 Booster and Storage Ring Magnet System and Power Supply

Magnetic elements of booster include 48 dipoles, 72 quadrupoles and 60 sextupoles. Dipoles are of C-type, curved with parallel ends. Each of them is of 1 m long and bending angle is of 7.5°. Two types of quadrupoles are planned to use. They are of 0.3 m long each and bore diameters are of 60 mm and 120 mm. The maximum gradient is of 18 T/m. Sextupoles are of 0.15 m long with bore diameter 110 mm and strength $1/2\ B'' = 50\text{T/m}^2$.

The superconducting magnetic elements of tau-charm storage ring include quads in two micro-beta insertions and 4 dipole wigglers in each ring. The warm magnetic elements of storage ring include 160 dipoles, 8 vertical bending magnets, 8 Robinson wigglers, 234 quadrupoles and 112 arc sextupoles. The length of bending magnet of a regular cell is of 1.08 m and bending radius is of 11.5 m. Dipoles are laminated from iron sheets of 440× 550 mm size, the gap of 60 mm. To make manufacturing easier dipoles are planned to be rectangular and the value of sagitta is added to pole width. Shims are foreseen to decrease pole width. The ends of dipoles have special profile to be effective length the same when changing magnetic field and to compensate fringing field effects.

Special attention has been paid to unification of quadrupoles under their design to reduce the cost of their manufacturing and operation. All quadrupoles except micro-beta ones are of the same type with two modification in winding. Quadrupoles are of 0.4 m long each with maximum gradient of 18 T/m and bore diameter 75 mm. Sextupoles are

		Monochrom. scheme	Standard Var.1	scheme Var.2
Energy, GeV	E	2.0	2.0	2.0
Luminosity, $cm^{-2}sec^{-1}$	L	$8.0 \cdot 10^{32}$	$9.2 \cdot 10^{32}$	$9.4 \cdot 10^{32}$
C.M. energy resolution, MeV	σ_w	0.14	1.8	2.4
Circumference, m	C	378	378	378
Natural emittance, nm	ϵ_0	15.1	388	393
Damping partition numbers	$J_x/J_y/J_\epsilon$	2/1/1	0.59/1/2.41	1/1/2
Bending radius in arc, m	ρ	11.5	11.5	11.5
Damping times, msec	$\tau_x/\tau_y/\tau_\epsilon$	19/39/39	43/25/11	19/19/9.7
Momentum compaction	α	$7.85 \cdot 10^{-3}$	$1.63 \cdot 10^{-2}$	$1.63 \cdot 10^{-2}$
Energy spread	σ_E	$7.18 \cdot 10^{-4}$	$6.23 \cdot 10^{-4}$	$8.50 \cdot 10^{-4}$
Total current, mA	I	441	516	536
Number of bunches	k_b	30	30	30
Number of particles in bunch	N_b	$1.2 \cdot 10^{11}$	$1.4 \cdot 10^{11}$	$1.4 \cdot 10^{11}$
RF voltage, MV	V	5	8	16
RF frequency, MHz	f_{RF}	476	476	476
Harmonic number	q	600	600	600
Bunch spacing, m	S_b	12.6	12.6	12.6
Energy losses per turn, keV	U_0	131	200	262
Bunch length, mm	σ_s	7.83	7.74	7.47
Longitudinal impedance, Ohm	$\lvert Z_n/n \rvert$	0.18	0.24	0.42
Beta functions at I.P., m	β_x^*/β_y^*	0.01/0.15	0.30/0.01	0.30/0.01
Vertical dispersion at I.P., m	D_y^*	0.36	0.	0.
Beam-beam parameters	ξ_x/ξ_y	0.040/0.029	0.04/0.04	0.04/0.04

Table 2: List of parameters of tau-charm collider

	N	AC A	DC A	R mΩ	L mH	Power kW
Dipoles	48	585	865	11	6.0	1700
Quads I	36	565	865	10	1.8	1200
Quads II	36	565	865	3	0.23	300
Sext. I	30	86	140	8.4	1.6	30
Sext. II	30	115	185	8.4	1.6	40

Table 3: Booster Power Supply Data

of 0.2 m long each with bore diameter 110 mm. The maximum strength for conventional scheme (high emittance lattice) is of 1/2 B″ =90 T/m^2.

The technology of manufacturing of magnetic elements is the same for booster and storage ring. The elements are manufactured from electrical die steel sheets. This technology provides good quality and reproducibility along with relatively low cost. Booster magnetic elements are planned to manufacture from cold-rolled isotropical steel of 2411 type and thickness of 0.5 mm. The most of the storage ring magnetic elements will be manufactured from steel of type 2212 and thickness of 1.5 mm.

The booster works during 73 s with repetition rate 25 Hz. It stops for 12 min when the tau-charm detector is switched on. The resonant scheme for booster power supply is adopted. Booster magnetic elements are excited by dc-biased sinewave current. The compensation of the pulse loss is realized by the separate reactors from the special pulse power supplies. There will be separate power supplies for dipoles, two quadrupole families and two sextupole families. Feedback and variable inductance in quadrupole circuits allow to keep constant the ratio of magnetic field to gradient during acceleration with accuracy of 0.1% . To reduce the voltage in power supplies the magnetic elements in dipole and quadrupole circuits are divided in groups and Whiete Circuit circular schemes are adopted. There are 6 such groups in dipole circuits and 2 groups in quadrupole circuits. The self-inductance coefficient ratio of isolation reactors to dipole ones is adopted to two. The source for dc-bias dipole is inserted in the reactor windings. The design data of the booster power supply are presented in Table 3.

Magnetic elements of storage ring are divided in 48 groups for the power supply. Each group consists of the identical magnetic elements (for example dipoles of dispersion suppressor) and has a separate power source. The prototype of the power source is DC sources that have been designed at the Institute of Electrophysical Apparatus (St.Petersburg) and manufactured at the "Electrotechnic" firm (Tallin, Estonia). The parameters of this power sources allow to get the driving range 0.6-1.0 of their nominal values with stability coefficient $\pm 10^{-}5$ in time running.

6 Vacuum System

The beam-particle bremsstrahlung in the residual gas atmosphere contributes to the beam lifetime. For the residual gas composition 70% H_2, 20% CO, 10% CO_2 and the pres-

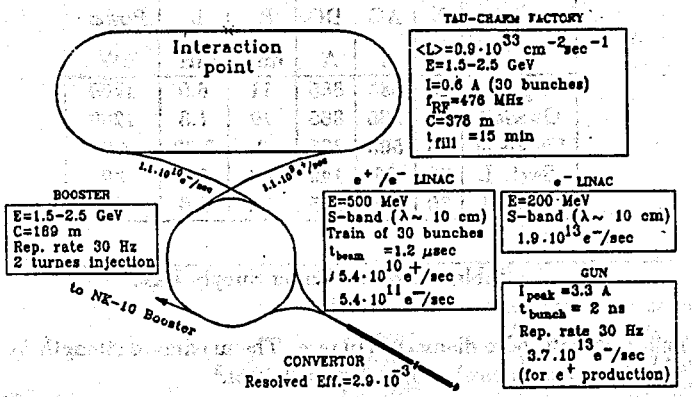

Fig. 1. Layout and structure scheme of tau-charm factory.

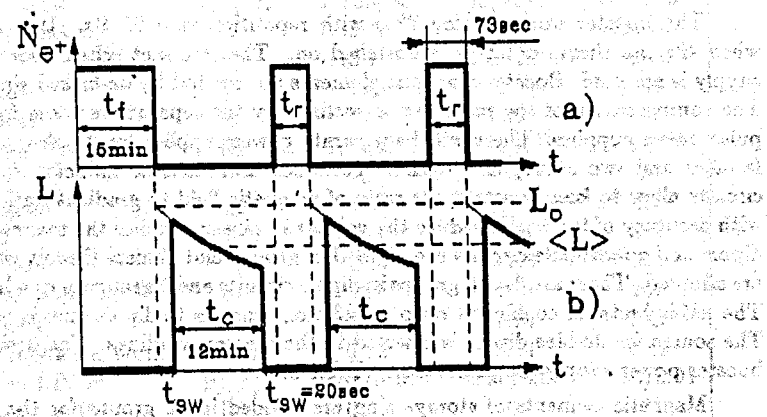

Fig. 2. The injector complex cyclograms: positron flux N_{e^+} from the injection complex (a) and the luminosity variation (b):

t_f - the positron "full-fill" time;

t_r - the refilling time;

t_c - the counting time;

t_{sw} - the detector switch on/off time;

<L> - the average luminosity.

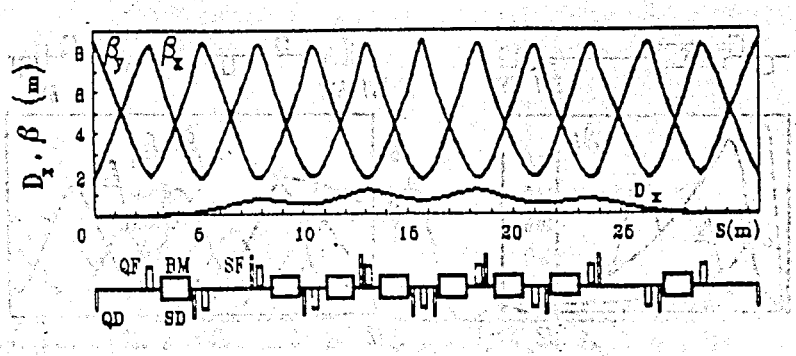

Fig. 3. Lattice functions in the booster superperiod.

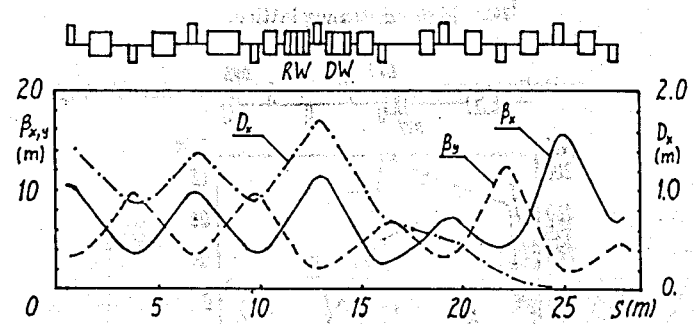

Fig. 4. Lattice functions in a regular cell and dispersion suppressor of high emittance lattice.

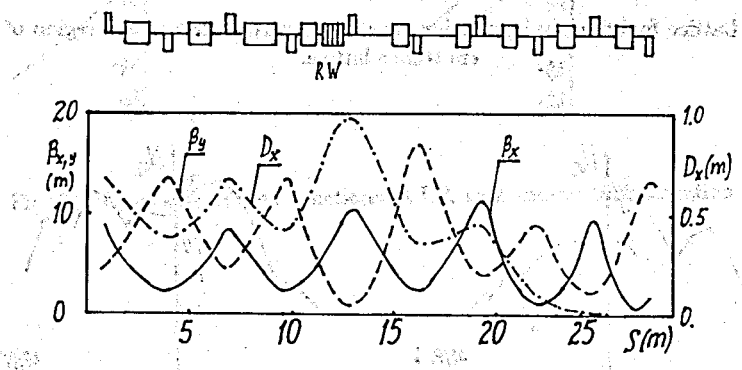

Fig. 5. Lattice functions in a regular cell and dispersion suppressor of low emittance lattice.

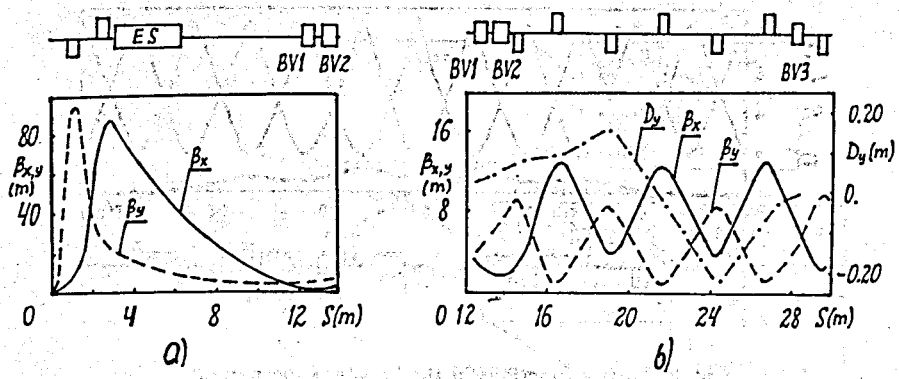

Fig. 6. Lattice functions in interaction region (a) and vertical separation region (b) of high emittance lattice.

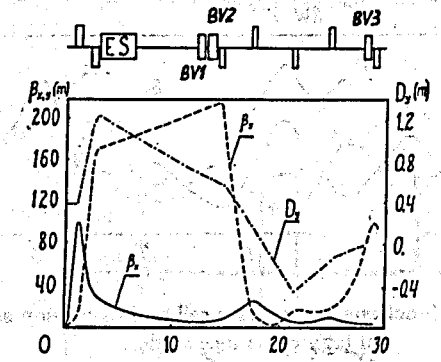

Fig. 7. Lattice functions in interaction region and vertical separation region of low emittance lattice.

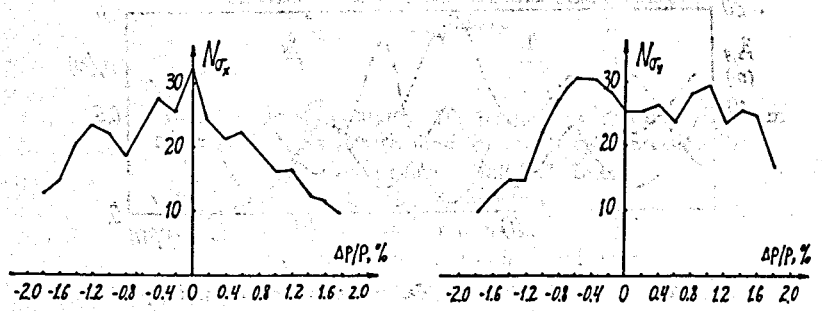

Fig. 8. Horizontal (a) and vertical (b) acceptances, expressed in sigma's, depending on momentum deviation.

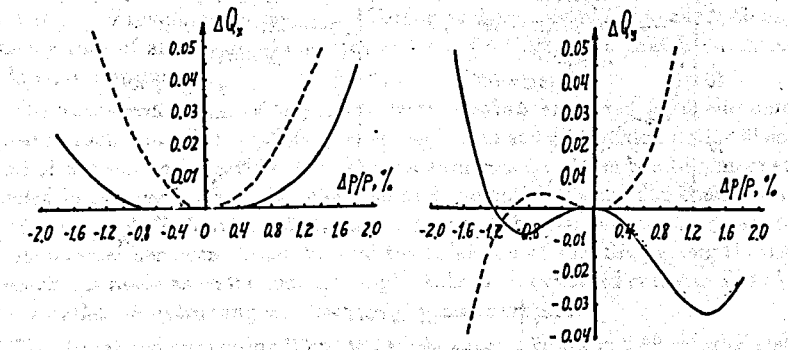

Fig. 9. Variations of tunes with momentum deviation.

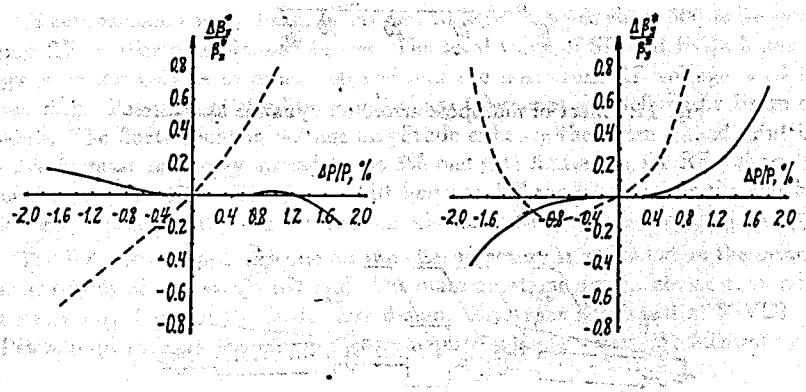

Fig. 10. Variations of beta functions at I.P. with momentum deviation.

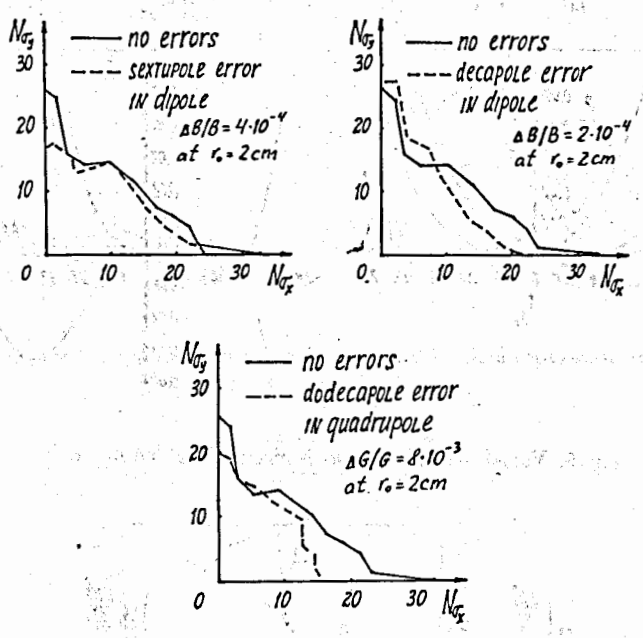

Fig. 11. Effect of multipole errors on dynamic aperture.

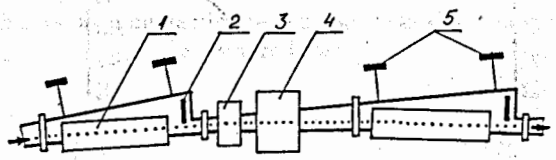

Fig. 12. Periodic cell scheme (1-dipole, 2-SR absorber, 3-sextupole, 4-quadrupole, 5-pumps)

sure of $2\cdot10^{-9}$ Torr vacuum lifetime is about 63h. The longitudinal acceptance using for beam lifetime estimates in this section adopted to be 1.5 % as conservative value. The gas loading is defined mainly by synchrotron radiation (SR) desorption. The photodesorption coefficient is adopted to be equal to $\eta = 10^{-6}$ [mol/phot], that corresponds to the dose of 50 A·h [11]. Providing the chemical cleaning and heating of the vacuum chamber the outgassing rate of aluminium doesn't exceed g= 10^{-9} [m·Pa/s], that is much less than stimulated desorption.

The vacuum chamber of tau-charm factory is manufactured from aluminium and designed in such a manner that SR goes through next straight section and is absorbed at the end of bending magnet (Fig. 12). The vacuum volume at the bending magnet region is devided in two parts: the beam chamber and the antichamber. The chamber aperture is 49×64 mm and it isn't varied along the arc length. The gap between the beam chamber and antichamber has been chosen to fulfil the condition of 95% SR passing through. The SR absorber is made as water-cooling coupler tube with extended surface. The absorbers have the outlet SR extracting windows for the user purposes.

The stimulated outgassing per a bending magnet is equal to $8\cdot10^{-8}$ [m^3·Pa/s]. Using the combined pumps with the pumping speed 0.4 m^3/s, one gets the pressure about $2\cdot10^{-7}$Pa at the absorber location. The additional pump is used for the pumping of the remaining part of vacuum volume and provides the pressure at the level of $2\cdot10^{-8}$ Pa.

7 RF System

To compensate energy beam losses and to keep bunches short 500 MHz superconducting RF cavities it is planned to use. The total value of SR and HOM losses at the energy E = 2.0 GeV is of order 300 kW and the maximum RF voltage is of 16 MV for one ring. The voltage amplitude and phase tolerances are defined by beam quality demands. The fluctuations in voltage amplitude enhance the beam spread. Putting the tolerable increase in energy spread to be 5% one gets limitation for RF voltage fluctuations $\Delta V/V \leq 5\cdot10^{-3}$. The phase shift between RF modules excites the synchrotron oscilations. Putting restriction for their amplitude to be $\leq$1 mm, one gets $|\delta\phi,| \leq 1°$.

The RF power supply scheme for tau-charm factory is grounded on the principle of separate supply of each cavity like [12]. The main questions are the choice of an adequate final stage amplifier and the feeder line design. Klystrons developed at "SVETLANA" (St.Petersburg) satisfied tau-charm factory requirements and have the following parameters:

-output power, kW - 80
-frequency, MHz - 500
-efficiency, % - 58
-amplification, dB - 45
-collector voltage, kV - 16
-collector current, A -8.6.

Each feeder line includes a ferrite circulator with a ballast load, that allows to refuse from phase shifter using. The effective automatic phase control is provided by the electronic phase shifter in a preliminary stage of a RF amplifier. The main coaxial feeder

connecting the circulator output and the cavity input has the cross section dimensions of 160 x 70 mm and the wave impedance of 50 Ohm. Thus, the RF power supplier consists of 4 independent RF lines with the total output power of 320 kW.

References

[1] V. S. Alexandrov et. al. , "JINR Tau-Charm Factory Design Considerations", Proceedings of IEEE Particle Accelerator Conference, San Francisco, Calif. , 1991, v.1, p.195.

[2] E. A. Perelstein et. al. , "JINR Tau-Charm Factory Study", Proceedings of XV International Conference on High Energy Accelerators, Hamburg, (1992).

[3] Paul Beloshitsky, "A Magnet Lattice for a Tau-Charm Factory Suitable for Both Standard Scheme and Monochromatization Scheme", LAL-RT/ 92-09, Orsay (1992).

[4] A. Faus-Golfe and J. Le Duff, "A Versatile Lattice for a Tau-Charm Factory That Includes Monochromatization Scheme", LAL-RT/92-01, Orsay (1992).

[5] Alexander Zholents, "Polarized J/ψ Mesons at a Tau-Charm Factory with a Monochromator Scheme", CERN SL/92-27 (AP), (1992).

[6] ESRF Foundation Phase Report, Grenoble 1987, pp. 225-247.

[7] V. P. Belov et. al. , "Injection Systems of Booster and Tau-Charm Factory", Proceedings of the Workshop on JINR c-tau Factory, 27-29 April 1993, JINR, Dubna.

[8] P. F. Beloshitsky, "Chromaticity Correction in JINR Tau-Charm Factory High Emittance Lattice", Proceedings of the Workshop on JINR c-tau Factory, 27-29 April 1993, JINR, Dubna.

[9] F. Scmidt, "Sixtrack, Version 1.1, Single Particle Tracking Code Treating Transverse Motion with Synchrotron Oscilations in a Sympletic Manner, User's Reference Manual", CERN/SL/91-52(AP),(1992).

[10] M. V. Danilov et. al. , "Conceptual Design of Tau-Charm Factory in ITEP", Proceedings of XV International Conference on High Energy Accelerators, Hamburg, (1992).

[11] M. Bernardini, "Vacuum System for ELETTRA of Synchrotron Trieste", Proceedings of the SR Vacuum Workshop, Wako-shi, Saitama, Japan, 1992, p.272.

[12] B. Barish et. al. , "Tau-Charm Factory Design", SLAC-PUB-5180, Stanford, (1990).

Received by Publishing Department
on October 10, 1993.